Transitions of the 3D Medial Axis under a One-Parameter Family of Deformations

Peter Giblin[1] and Benjamin B. Kimia[2]

[1] Department of Mathematical Sciences,
The University of Liverpool, Liverpool, England L69 3BX
pjgiblin@liv.ac.uk
[2] Division of Engineering, Brown University,
Providence, RI, USA
kimia@lems.brown.edu

Abstract. The instabilities of the medial axis of a shape under deformations have long been recognized as a major obstacle to its use in recognition and other applications. These instabilities, or *transitions*, occur when the structure of the medial axis graph changes abruptly under deformations of shape. The recent classification of these transitions in 2D for the medial axis and for the shock graph, was a key factor both in the development of an object recognition system and an approach to perceptual organization. This paper classifies generic transitions of the 3D medial axis, by examining the order of contact of spheres with the surface, leading to an enumeration of possible transitions, which are then examined on a case by case basis. Some cases are ruled out as never occurring in any family of deformations, while others are shown to be non-generic in a one-parameter family of deformations. Finally, the remaining cases are shown to be viable by developing a specific example for each. We relate these transitions to a classification by Bogaevsky of singularities of the viscosity solutions of the Hamilton-Jacobi equation. We believe that the classification of these transitions is vital to the successful regularization of the medial axis and its use in real applications.

1 Introduction

The practical use of the medial axis in visual tasks such as object recognition, perceptual grouping, shape modeling and tracking, etc. is adversely affected by the frequent and omni-present instabilities of the medial axis under deformations of shape. Previous approaches have either embedded an implicit regularization in the detection process [11,16] or have explicitly included a post-processing "pruning" mechanism [13,15] an alternative to reducing the effect of the medial axis instability is to utilize this instability to represent shape deformations: each deformation sequence can be broken into a series of contiguous deformation segments, where the medial axis topology does not change, connected by the transition point itself. This annotation of a shape deformation by the medial axis transitions, or discretization of a continuous path into a set of discrete descriptors, has been key in the development of object recognition and perceptual

A. Heyden et al. (Eds.): ECCV 2002, LNCS 2351, pp. 718–734, 2002.

grouping approaches using the medial axis in 2D [10,14]. This paper investigates the transitions of the medial axis in 3D.

The transitions of the 2D Medial Axis under a one-parameter family of deformations were derived in [6] using results from transitions of the symmetry set [4]. These consist of two transitions, A_1A_3 and A_1^4, as shown in Figure 1. The notation A_n^k implies k-fold tangency of order n, *i.e.*, A_1^2 indicates the most generic situation of a circle tangent at two places each with regular tangency, A_1^3 indicates a circle tangent at three places each with regular tangency, and A_3 indicates a circle tangent at a curvature extremum. The three types A_1^2, A_1^3, and A_3 are the only generic forms of the medial axis in 2D [8], while generic transitions under a one-parameter family of deformations are the A_1A_3 and A_1^4 transitions. The A_1A_3 transition occurs frequently due to boundary noise and is recognized as one of the classical instabilities of the medial axis. This transition is the result of formation of a bump on the boundary of the shape which initially bends the medial axis, but when it grows in size it will eventually "break" the axis leading to the growth of a new branch, Figure 1. The second medial axis transition, the A_1^4 transition, occurs when a smooth A_1^2 curve segment on the medial axis between two A_1^3 points shrinks to a point so that the combination of two three-contact A_1^3 points leads to a single four-contact A_1^4 point (this is generic only in a family of curves), Figure 1 . As the shape is compressed along the direction of the central A_1^2 curve, this curve shrinks so that eventually its A_1^3 end-points overlap, as in the fourth figure in the bottom row of Figure 1, the A_1^4 transition. Additional deformations of the shape will form a new A_1^2 axis by swapping the pairing of the four branches coming into the A_1^4 points.

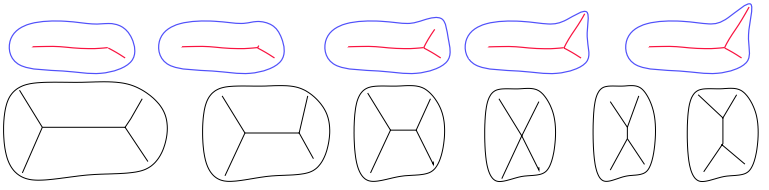

Fig. 1. (Top) The A_1A_3 transition: the formation of a bump initially bends the related portion of the medial axis, however, as the bump grows, at some point the axis forms a discontinuity, the A_1A_3 transition after which a new axis grows at this point. (Bottom) The A_1^4 Transition: changes in the aspect ratio of a shape, *e.g.*, as caused by compressing it along a certain direction, can cause the central portion of the medial axis to shrink to a point (A_1^4 contact). Further deformation causes the growth of another axis in the center. The transition itself can mediate the process of making the two sets of shapes on either side equivalent.

The derivation and a complete classification of these transitions, which are the *instabilities* of the medial axis, or its variant the shock graph, is significant in many ways. For example, successful recognition relies on an understanding of these points of instability so that the resulting medial axis graphs on either side of the transition, which have different structures, can be explicitly related. In

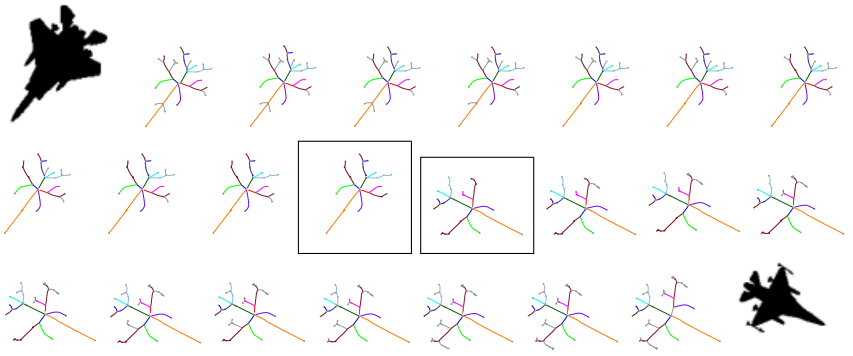

Fig. 2. The key role of characterizing the medial axis transitions in a 2D object recognition approach is highlighted. An arbitrary deformation sequence from one shape to another is described by the set of transitions the medial axis experiences. This "discretization" relies on the instabilities of the medial axis to reduce the search space for finding the optimal deformation path to a practical range. Results of the optimal sequence for a pair of planes are shown [14].

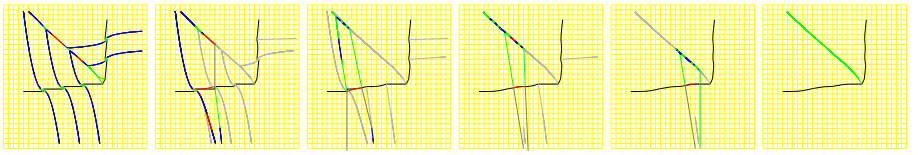

Fig. 3. The smoothing of the "L-shape" with noise and the square retain the coarse scale boundary singularity (corner of the L) while removing the noise [17].

the approach described in [14] an equivalence relation is defined for all shapes with the same shock graph topology, and another equivalence relation for all deformation paths with an identical sequence of transitions. Shape similarity is defined as finding the least action deformation path, where costs are associated with each deformation segment between transitions. Thus, the problematic medial axis instabilities are in fact used to advantage to effect stable recognition, Figure 2.

These transitions are also of critical value to perceptual grouping operations [10]. Specifically, note that the smoothing of a boundary can be achieved by deforming a shape to a neighboring transition. For example, since small perturbations cause growth after the A_1A_3 transition, one can remove branches which likely arose in this manner by retaining an A_1A_3 transition at that point [17], Figure 3. Other group operations are described in [10].

The Local Form of 3D Medial Axis: The goal of this paper is to study the transition of the medial axis of a 3D shape. The local form of the medial axis points was classified into five types [7] based on the order of contact of the corresponding sphere of tangency. The most typical example of a medial axis point is the centers of ordinary bitangent spheres, A_1^2 points. These A_1^2 points

organize as sheets with other neighboring A_1^2 points. Less frequently, some medial axis points have spheres which are tangent at three points, A_1^3 points. These organize into curves with neighboring A_1^3 points, and often represent the central axis of the shape. Note that the A_1^3 curves are at the intersection of three A_1^2 sheets. Another possibility is for the two A_1^2 points to coincide to form an A_3 curve, the *rim* curve, which bounds a single A_1^2 sheet and corresponds to a *ridge* on the surface. Much less frequently, some MA points may acquire four points of tangency, A_1^4 points. These are generic, in contrast to five points of tangency or higher which disappear with small perturbations of the shape. The A_1^4 points are isolated from other A_1^4 points, and form from the intersection points of six A_1^2 sheets and four A_1^3 curves. Finally, some MA points are centers of spheres with regular A_1 tangency at one point, and a higher-order A_3 contact at another, as denoted by the A_1A_3 notation. These points are isolated from other A_1A_3 points, but both end at an A_1A_3 point. These five types of MA points, namely A_1^2 (sheets), A_1^3 and A_3 (curves), and, A_1^4 and A_1A_3 (points) are the only generic types of MA points in 3D.

Overview : We approach the problem of classifying the transitions of the medial axis in 3D in two distinct ways. First, in Section 2 we examine how a generic medial axis point can acquire additional non-generic contact by studying possible interactions between each pair of generic medial axis types. Some interactions can never occur, while others lead to transitions which are shown to be viable by creating an example. Second, in Section 3 we relate these transitions of the 3D medial axis to a classification of the singularity of viscosity solutions of Hamilton-Jacobi equations. Finally, in Section 4 we describe examples for each transition and illustrate its formation in a sequence of deformations.

2 Description of the Transitions of Medial Axes in 3D

In this section we shall describe how the possible transitions of generic 1-parameter families of medial axes in 3D can be enumerated. The list we produce is motivated by the work of Bogaevsky [2,1] and in Section 3 we give a brief indication of the connection between his work and our list[1].

We can approach the listing from several perspectives; first let us consider the concept of **specialization**. If one singularity type, such as A_1^2, *specializes* to another, such as A_3, this means that in a general family we can have a sequence of A_1^2 singularities which, in the limit, becomes A_3. Equivalently, we can perturb an A_3 by an arbitrarily small amount so that it yields A_1^2. We write $A_1^2 \to A_3$ or $A_3 \leftarrow A_1^2$. This specialization can indeed occur: as the two points of contact of a bitangent sphere tend to coincidence, so the limit of these points of contact is a ridge point of the surface (and in fact the line joining the points of contact has for its limit a principal direction at the ridge point [5]). On the other hand, A_1^3

[1] It needs to be said here that technical difficulties, which are at present under active consideration, make it impossible for us to be completely precise about the meaning of 'generic' and about the equivalence relation which implicitly underlies our finite list of pictures. However, there is no doubt that all cases have been considered and there is no transition which 'looks' different from those we present here.

does not specialize to A_3, or, putting it the other way round, we cannot perturb an A_3 by an arbitrarily small amount so as to achieve A_1^3.

Another principle which we need is that in a 1-parameter family of surfaces we can expect singularities to occur which are of one higher codimension (order of complexity) than those occurring for a single surface. Those for a single surface are $A_1^2, A_1^3, A_1^4, A_3 and A_1A_3$ and for a family of surfaces this list will be augmented by singularities only involving A_n^k with odd n and codimensions (sum of suffixes) adding to 5, (continuing to use the standard Arnold's notation for singularities, as described for example in [3]):

$$A_1^5, A_1^2A_3, A_5, D_5,$$

but D_5, whose "normal form" as a function of two variables is $x^2y + y^4$, is not a local minimum, so does not occur in the medial axis context. Note that we might also expect earlier singularities to produce new phenomena. The specializations relevant to the present situation are then:[2]

$$\begin{array}{ccccccc} A_1 \to A_1^2 & \to & A_1^3 & \to & A_1^4 & \to A_1^5 \\ \downarrow & & \downarrow & & & \\ A_3 \to A_1A_3 & \to & A_1^2A_3 & & & \\ & & \downarrow & & & \\ & & A_5 & & & \end{array}$$

From this, other specializations can be deduced, for example when we perturb $A_1^2A_3$ we can expect to find A_1A_3 (since $A_1 \to A_1^2$) and also (for a different perturbation) A_1^4 (since $A_1^2 \to A_3$).

The second approach is via the **geometry** of the situation. When one or more singularities coalesce to a more complex one (as with $A_1^3 \to A_5$) we can ask how this happens geometrically. A useful result in this direction is the following.

Proposition 1 Let γ be a point of the medial axis of the surface M at which the singularity is of the simplest kind, A_1^2, so that the medial axis is *smooth* at γ. We can therefore consider a sufficiently small neighborhood U of γ in 3-space, contained within the maximal ball D (solid 3-sphere) whose center is γ, and intersecting the medial axis in a smooth surface S. Then U does not contain any points of the medial axis of M besides those in S. This means that A_1^2 singular points do not coalesce with others in making a more complex singularity: other points of the medial axis cannot approach a smooth A_1^2 point in order to 'collide' with it.

Proof. Let γ^+ be one of the points of contact of the bitangent sphere centered at γ and let p be a point on the radius of this sphere from γ to γ^+ other than γ itself. Suppose p is on the medial axis; then it is the center of a maximal ball D'. This ball D' cannot have the point γ^+ in its interior since D' would then

[2] A convenient way to visualize these specializations is to think of functions of one variable, $y = f(x)$, with an A_k singularity being a $k+1$ fold root, and A_kA_l meaning both a $k+1$ fold and an $l+1$ fold root of the same function. Thus A_5 represents a 6-fold root which can be perturbed for example into three 2-fold roots: $A_5 \leftarrow A_1^3$, but not into four 2-fold roots: A_1^4 does not specialize to A_5.

contain points outside M. In that case D' must be small enough to be entirely inside D, and of radius strictly smaller than the radius r of D. It follows that the points where the boundary sphere of D' is tangent to M must also be strictly inside D, which is impossible since D is maximal. It now follows that all the radii outwards from *smooth* points of the medial axis near γ fail to contain points of the medial axis other than the points of the smooth A_1^2 sheet near γ. But over a smooth piece of the medial axis the boundary retracts to the medial axis along the radii, so these radii fill out a neighborhood of γ in the surrounding 3-space, and this completes the proof. ∎

We note that the same approach used to isolate an A_1^2 point from other medial axis points can be applied in other situations: again, the radii out from medial axis points γ to points of contact γ^+ will be free from other medial axis points. For example, two A_1^3 curves cannot normally meet, but they can if they lie on the same sheet of the medial axis: they can then approach and become tangential. Similarly, A_3, A_1A_3 and A_1^4 points can only be "approached" along sheets of the medial axis through them, not through the "empty space" between the sheets.

We can now make a list of the possible transitions on medial axes in 3D, with some commentary on each one. We envisage these as two singularities " coalescing" or "colliding" and use the specialization method to reduce the number of possibilities.

Collisions involving A_3: In this and the other tables, the third singularity is the simplest one which is a specialization of both colliding singularities $\mathcal{A}$ and $\mathcal{B}$.

$\mathcal{A}$	$\mathcal{B}$	$\mathcal{C} \leftarrow \mathcal{A}$ and $\mathcal{C} \leftarrow \mathcal{B}$	See note
A_3	A_3 or A_1A_3	A_5	(1)
A_3	A_1^3	A_1A_3 [type II]	(2)
A_3	A_1^4	none—see above	

Note (1). Two A_3 curves could in principle collide by moving in a common sheet of the medial axis, but since the contact points must remain on opposite sides of the collision this would imply A_3^2 at the transition, and this is not one of our viable list of singularities.

Note (2). At the moment of collision the A_3 and A_1^3 curves must be tangential, something that only happens generically for a family of surfaces. The condition for this can be expressed in terms of the principal curvatures at the A_3 point, the derivative of one of these and the position of the other contact point, using formulae of [5], but the result does not seem to be enlightening.

Other collisions involving A_1^3:

$\mathcal{A}$	$\mathcal{B}$	$\mathcal{C} \leftarrow \mathcal{A}$ and $\mathcal{C} \leftarrow \mathcal{B}$	See note
A_1^3	A_1^3	A_1^4	(3)
A_1^3	A_1^4	A_1^5	
A_1^3	A_1A_3	$A_1^2A_3$ [type II]	

Note (3). The two A_1^3 curves must be tangent at the moment of collision. The tangent to an A_1^3 axis passes through the circumcenter of the triangle through

the three contact points [5] so this implies that the four contact points for A_1^4 will be *coplanar*.
Other collisions involving A_1^4:

$\mathcal{A}$	$\mathcal{B}$	$\mathcal{C} \leftarrow \mathcal{A}$ and $\mathcal{C} \leftarrow \mathcal{B}$	See note
A_1^4	A_1^4	A_1^5	
A_1^4	A_1A_3	$A_1^2A_3$[type I]	

Other collisions involving A_1A_3 Here $\mathcal{C} = A_5$ although as we shall see, the A_1A_3 transition itself can produce two A_1A_3 singularities.

Table 1. A summary of the transitions of the medial axis arising from the interaction of generic types presented in two distinct ways.

$\mathcal{A}$	$\mathcal{B}$	$\mathcal{C} \leftarrow \mathcal{A}$ and $\mathcal{C} \leftarrow \mathcal{B}$
A_3	A_3 or A_1A_3	A_5
A_3	A_1^3	A_1A_3-II
A_1^3	A_1^3	A_1^4
A_1^3	A_1^4	A_1^5
A_1^3	A_1A_3	$A_1^2A_3$-II
A_1^4	A_1^4	A_1^5
A_1^4	A_1A_3	$A_1^2A_3$-I
A_1A_3	A_1A_3	A_5, A_1A_3-I, A_1A_3-II

Transition	Collision of Types
A_1^4	A_1^3 - A_1^3
A_1^5	A_1^4 - A_1^4, A_1^4 - A_1^3
A_5	A_1A_3 - A_1A_3, A_3 - A_3
$A_1A_3 - I$	A_1A_3 - A_1A_3
$A_1A_3 - II$	A_1A_3 - A_1A_3, A_1^3 - A_3
$A_1^2A_3 - I$	A_1^4 - A_1A_3
$A_1^2A_3 - II$	A_1^3 - A_1A_3

In summary, there are seven transitions which could possibly arise, Table 1. In Section 4 we show that the transitions do indeed arise in all cases by constructing an example for each. However, we first relate these to the singularity classification results of Bogaevsky in Section 3.

3 Relationship with the Work of Bogaevsky

In [2,1], I.A. Bogaevsky examines several related problems connected with the classification of transitions (perestroikas) of "minimum functions". That is, we consider a local family of functions of the form $F(t, \mathbf{x}) = \min f(t, \mathbf{x}, \mathbf{y})$ where t is a "time" parameter (so a single real parameter), $\mathbf{x} \in \mathbf{R}^3$ and $\mathbf{y}$, over which the minimum is taken, is in a Euclidean space which for the medial axis application would be 2-dimensional, corresponding to the 2-dimensional surface whose medial axis is being considered. For each value of t close to some t_0 (the moment of transition) we can consider the set X of points $\mathbf{x}$ for which F is not differentiable. It is this set which is pictured as it evolves through the transition. Bogaevsky provides a complete list of these transitions, provided the function f is generic. The pictures which we reproduce are in Figure 4 from [1].

There are also two special cases considered. The first one, described as " shocks" (these are not the same as the shocks which we associate with a dynamical construction of the medial axis) is one to which an "arrow of time" can be associated, where in fact the local topology of the set X as above is "trivial"

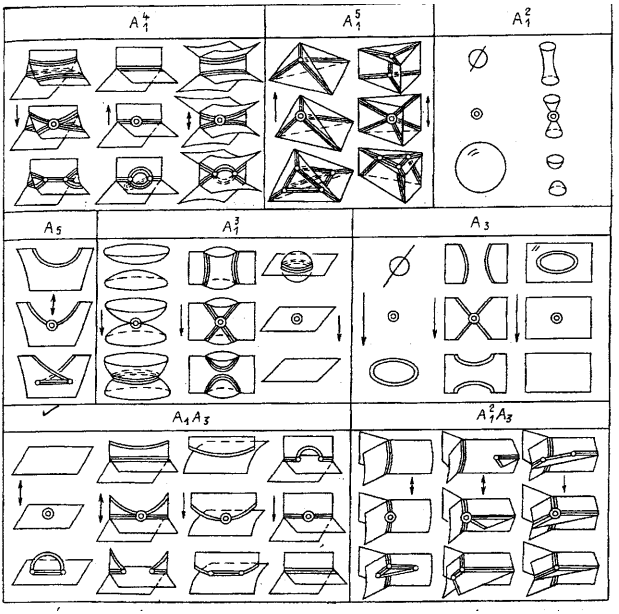

Fig. 4. From [1]. The 26 topologically different of perestroikas of the momentary shock waves are shown by arrows. Those relevant to the medial axis are those shown by double arrows. Single lines indicate the boundary of the depiction, double lines indicate rims, A^3 curves on the medial axis which correspond to ridges on the surface, and triple lines indicate A_1^3 curves. Concentric circles indicate an overlap of medial points.

(homotopic to a point) for all $t \geq t_0$: we might say loosely that moving through the transition from $t < t_0$ to $t > t_0$ "simplifies the topology." The arrow of time is indicated on Bogaevsky's diagrams and those without an arrow are transitions where trivial topology is guaranteed only *at* t_0.

The second special case is the one which concerns us most closely. Here, the topology of X is trivial for all t close to t_0, and this corresponds to the well-known fact that the medial axis of a smooth compact connected surface is contractible to a point. The arrow of time can then go either way. It is indicated on the diagrams by a double arrow. The diagrams with a double arrow therefore represent all the transitions on the medial axis, possibly including some extras which cannot occur for surfaces, provided the family of distance functions is generic[3]. Thus in this situation we have a family of surfaces parametrized say by $\Gamma(t, \mathbf{y})$ where t is the 1-dimensional time parameter and $\mathbf{y}$ is 2-dimensional. We then define $f(t, \mathbf{x}, \mathbf{y}) = ||\mathbf{x} - \Gamma(t, \mathbf{y})||^2$. The usual medial axis is simply the

[3] A technical difficulty that has so far not been resolved is whether this is equivalent to studying the transitions of the medial axis for a generic 1-parameter family of generic surfaces. Previous examples where this problem has arisen (*e.g.,* the study of caustics by reflection) have been answered positively, but each case needs a separate, and rather lengthy investigation.

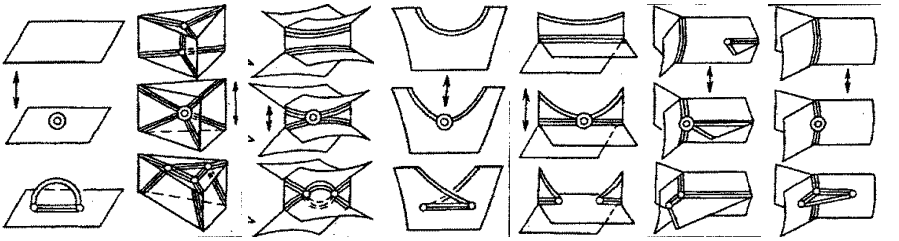

Fig. 5. A summary figure of those singularities (perestroikas) of the viscosity solution of the Hamilton-Jacobi equation, represented in Figure 4, that relate to the transitions of the medial axis in 3D.

set of points for which the corresponding minimum function (minimum over $\mathbf{y}$) is not differentiable. The singularities in Figure 4 involving double arrows are shown in summary form in Figure 5.

4 Examples and Illustrations

1) The A_1A_3-I Transition : Consider a medial axis sheet (A_1^2 points) arising from two boundary surfaces. An analogous deformation to that in Figure 1 is where one of the boundary surfaces is protruded to form a bump. A good example of a generic bump is a two-dimensional Gaussian with asymmetric sigmas, *i.e.*,

$$z = f(x,y) = Ae^{\frac{-x^2}{2\sigma_x^2}} e^{\frac{-y^2}{2\sigma_y^2}} \text{ where } \sigma_x < \sigma_y. \tag{1}$$

Since the high or principal curvature is along the yz plane, the medial axis sheet arises from the centers of curvature of the curve $z = f(x,0)$, whose curvature $\kappa(x)$ given by

$$\kappa(x) = \frac{f''(x,0)}{(1+f'(x,0)^2)^{\frac{3}{2}}} = \frac{A}{\sigma_x^4} e^{(\frac{-x^2}{2\sigma_x^2})} \left(x^2 - \sigma_x^2\right).$$

In particular, $\kappa(0) = \frac{-A}{\sigma_x^2}$. This implies that in the absence of additional structure, the Gaussian bump will form an A_3 point at $\left(0, 0, f(0,0) + \frac{1}{\kappa(0)} = A - \frac{\sigma_x^2}{A}\right)$. For a bump which is barely visible, the ratio of σ_x^2 to A is very high, *i.e.*, the spread of the protrusion is much larger than its magnitude. Thus, the center of curvature forms very far from the peak and the likely presence of any other structure typically prevents the formation of the A_3 point. As the salience of the bump increases in a one parameter family of deformations, the ratio $\frac{\sigma_x^2}{A}$ decreases until at some point, the (thus far non-maximal) sphere of curvature of the bump also forms a contact elsewhere, forming an A_1A_3 transition. This is parallel to the 2D case shown in Figure 1. From this point onward, the sphere is maximal and the corresponding medial point emerges, undisturbed by other structure. Figure 6

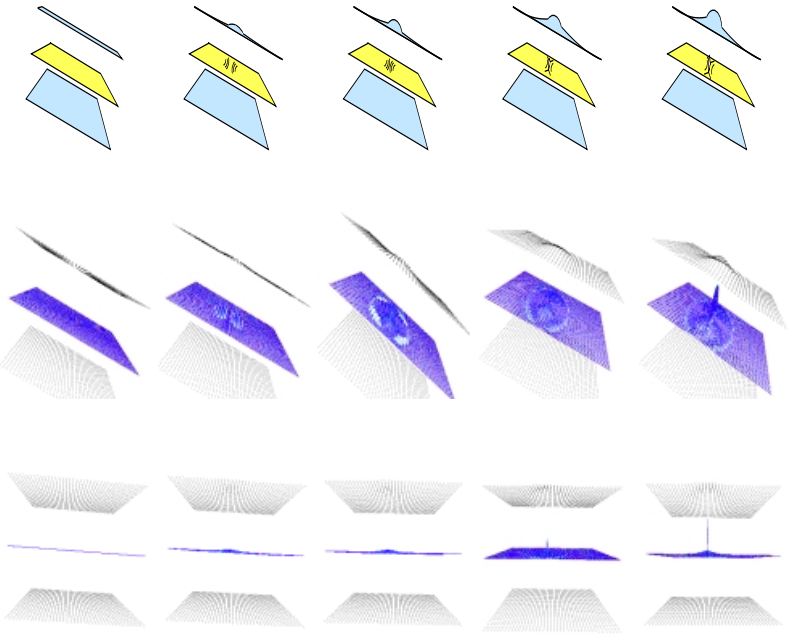

Fig. 6. The sketch (top row) and two simulated views of the A_1A_3-I transition, (Middle and Bottom rows).(Simulations from [12]).

shows a sketch of this transition, and a simulation with $\sigma_y = 2.5$, $\sigma_x = 1$ and a sequence of increasing A, shown from two different views.

2) The A_1^5 Transition: A second transition which also parallels the second 2D case shown in Figure 1 can be obtained by a shape deformation shrinking an A_1^3 curve segment with two four-contact A_1^4 end-points so as to obtain a five point contact A_1^5 point. Since six sheets and four curves come together at an A_1^4 point, the resulting A_1^5 has six A_1^3 curves and nine sheets: the common curve disappears from each leaving six in total; of the six sheets three are common to the two A_1^4 points leaving nine in total.

An example can be easily created by simply considering the polyhedral shape formed from the tangent planes at each of five points on a sphere, representing the shphere of contact at the A_1^5 transition shape. A perturbation of the five points so that they are no longer on a sphere, *e.g.,* by moving a point in or out of the sphere generates shapes on either side of the transition. Specifically, consider five points $\{p_1, p_2, p_3, p_4, p_5\}$ on a (unit) sphere and the planes T_i tangent to the sphere at $p_i = (x_i, y_i, z_i)$ represented by the normal vector $n_i = (\cos\theta_i \cos\phi_i, \sin\theta_i \cos\phi_i, \sin\phi_i)$, $i = 1, \ldots, 5$. Consider also $(\theta_i, \phi_i)\, \epsilon \{(0,0), (\frac{\pi}{2}, 0), (\frac{-\pi}{2}, 0), (0, \frac{\pi}{2}), (0, \frac{-\pi}{2})\}$. In this non-generic situation, the

skeleton has an A_1^5 point, but any small variation in these angles, leads to the generic situation with two A_1^4 points, Figure 7.

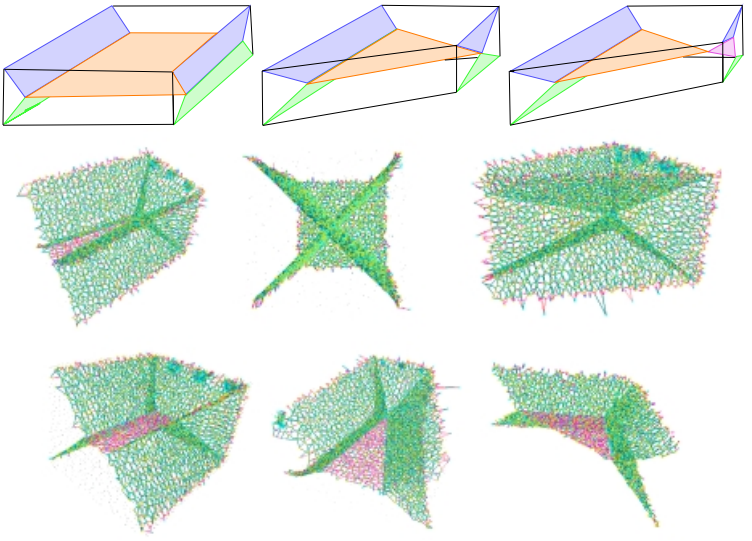

Fig. 7. A sketch and two views of the simulation of the A_1^5 transition.(Simulations from [12]).
Note that these simulations are hard to see for two reasons : *(i)* From each view, the 3D structure of interest is occluded by intervening structure, so that only an interactive 3D visualization is fully effective in perceiving this; *(ii)* The medial axis, which is computed from point cloud data, is noisy and needs to be regularized. Successful regularization of the medial axis requires an understanding of how it is affected by small perturbances, precisely the topic of the paper! We expect to apply the transitions derived here for regularization of the medial axis in the near future.

3)The A_1^4 Transition : In this transition two A_1^3 curves approach each other with tangent planes to their respective sheets aligned at the moment of collision. Each of the three contact A_1^3 points shares two points with the other so that at the transition we have a four point contact A_1^4 medial axis point. Beyond this point there is a topological split in the tangential plane, due to collision of the two A_1^3 curves, creating a gap in the middle of the two A_1^3 curves connected via a newly generated transversal sheet bounded by two new A_1^3 curves, ending at the two newly generating A_1^4 points on either end. An example can be created by deforming a cylinder with a roughly rectangular base, Figure 8. This could be generated by moving a rectangular shape, *e.g.*, as generated by say a superquadric, in the z direction, leading to two A_1^3 curves parallel to z-direction-axis. Now, to move the two A_1^3 curves towards each other, we can pinch a "waist" in the cylinder and decrease the size of the waist until transition point where the two A_1^3 curves become tangent at an A_1^4 point. With additional pinching two A_1^4 points move in opposite directions. Specifically, consider the 3D superquadric

$$\left(\frac{x}{a_1 f(z)}\right)^{\frac{2}{\epsilon}} + \left(\frac{y}{a_2 f(z)}\right)^{\frac{2}{\epsilon}} = 1, \text{where} \quad 0 < \epsilon < 2, 0 < a_1 < a_2, f(z) = \frac{z^2 - 1 + a_3}{a_3}, \tag{2}$$

so that at $z = \pm 1$ we have $f(z) = 1$,*i.e.,* the cross section is independent of the parameter a_3. We then vary a_3 to change the extent by which the tube is "squeezed", Figure 8.

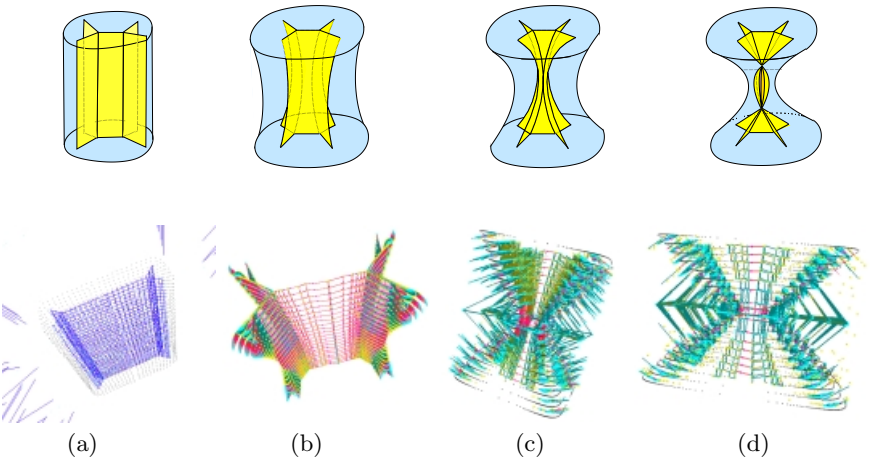

Fig. 8. Sketch and Example of Perestroika with an A_1^4 point.(Simulations from [12]).

4) The A_5 Transition : In this transition, in the course of a deformation sequence, two surface ridges approach each other and combine into one. Each ridge is manifested as an A_3 curve on the medial axis, terminating at an A_1A_3. A common A_1^3 axis connects the two ridges close to the A_5 transition. To create an example, one can initially use the A_1A_3 transition to generate a ridge and a corresponding A_3 medial curve hanging onto a newly generated A_1^3 curve. This can then be followed by a second A_1A_3-I transition to generate another ridge, and move the newly generated A_3 curve to split the existing A_1^3 curve via an A_1A_3-II transition, to arrive at the picture at the bottom of the A_5 transition, Figure 5.

It is interesting to approach this transition on the medial axis from the perspective of transition on ridges. These transitions have been studied extensively in [9]. The only transition of ridges which is manifested in the medial axis is the A_5 transition where two A_4 turning points approach to form the A_5, Figure 9. The segment of the ridge between the two A_4 turning points is not visible on the medial axis, in the sense that it does not give rise to maximal spheres. The portions of the ridge, which can be visible lead to two A_3 curves, which *must* each end in an A_1A_3 before the A_4 turning points are reached.

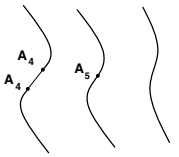

Fig. 9. The only transition of ridges which is manifested in medial axis: two A_4 turning points, bounding an "invisible" portion of the ridge approach each other and form an A_5 point at the transition. The entire ridge is visible after this point.

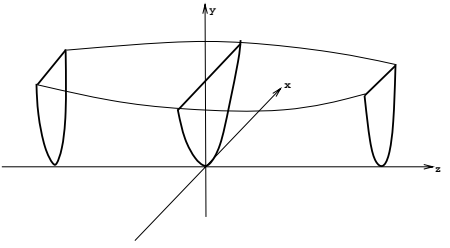

Fig. 10. Generating an A_5 transition shape which can then be perturbed to give shapes on either sides of the transition.

We can generate a shape with A_5 contact and perturb it to see the effect of changes at the A_5 transition. Consider the following graph of $f(x)$ and its curvature:

$$f(x) = x^2 + bx^3 + cx^4 + \cdots, \quad \kappa(x) = \frac{2 + 6bx + 12cx^2}{[1 + (2x + 3bx^2 + 4cx^3 + \cdots .)]^{\frac{3}{2}}}.$$

Thus, the distance of $(x, f(x))$ from the center of curvature $(0, \frac{1}{2})$ is

$$d^2(x) = x^2 + (x^2 + bx^3 + cx^4 + \cdots - \frac{1}{2})^2 = -bx^3 + (1-c)x^4 + 2bx^5 + (b^2 + 2c)x^6 + \cdots$$

To get an A_5 contact we need to have $b = 0$, $c = 1$, but a non-zero coefficient of x^6, which can be ensured by simply ignoring all higher order terms in $f(x)$ after x^4, since $b^2 + 2c = 2 \neq 0$.

We can now generate a 3D shape by translating this graph as a profile and slightly perturbing it to general shapes on either sides of the transition, Figure 10,

$$y^2 = x^2 + \left(\frac{z + a_1}{a_2}\right) x^3 + x^4.$$

The parameter a_2 when high enough ensures that near $z = 0$ the function behaves as $x^2 + x^4$. The parameter a_1=0 gives the transition shape, but perturbing a_1 to non-zero values should interfere with the formation of A_5 contact at $z = 0$.

We now construct an example where a ridge is added to an object which already has a "prominent" ridge using the transition shown in Figure 6. As the newly formed ridge approaches the existing ridge it "dissolves" into it, taking a new identity, as the left to right sequence in the A_5 transition sketched in Figure 11 illustrates. Specifically, the example is generated from a cylinder with an elliptical base which is "pinched" in the middle $\frac{x^2}{a_1^2} + \frac{y^2}{a_2^2} = \frac{z^2 - 1 + a_3}{a_3}$, where $a_1 > a_2$ controls the aspect ratio of the ellipse (eccentricity) and $a_3 \geq 1$ controls the size of the "waist", Figure 11(a). This formulation ensures that the $z^2 = 1$ level sets are the same as a_3 is altered.

Now, consider placing a "bump" near the ridge in the central portion, through an A_1A_3-I transition, Figure 11(b), as explained earlier. As the "bump" travels

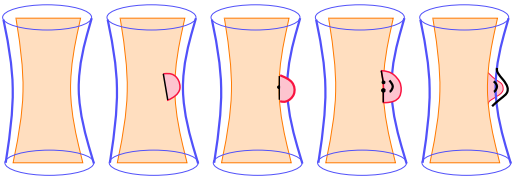

Fig. 11. The A_5 transition is a merging of two ridges into one. In this example we begin with an existing ridge (ridge of elliptical cylinder), create a new one (red tab), move it towards the original ridge until they merge.

towards the ridge, the rib corresponding to the ridge and the A_1^3 axis corresponding to the bump experience an A_1A_3-II transition, Figure 11(c). After this point, we have two situations, the top main ridge connected with the new ridge and similarly for the bottom main ridge, which are candidates for the A^5 transition. Note that the original ridge has somewhat flattened due to the nearby placement of the new bump. Thus, its effect is manifested in the A_3 axis on each side. Note that a requirement of the shrinkage of the A^3 axis in this transition is that the A_3 curve becomes tangent to it.

5) The A_1A_3-II Transition : In this transition two curves, one A_3 and one A_1^3, approach each other, become tangent, and then split into two portions each, grouped at the new A_1A_3 points. It is rather straightforward to generate examples for this transition: by "flattening " a ridge, its A_3 (rim) curve moves into the A_1^2 sheet it is on. If this sheet is bounded by an A_1^3 curve elsewhere, the A_3 and A_1^3 curves can eventually collide, Figure 12, top row. Alternatively, the ridge can be fixed and the "width" of the shape can be reduced, thus moving the A_1^3 curve closer to the A_3 curve, with the same effect. In the first case, we sweep a parabola along the z axis, widening it at $z = 0$, and closing it up with a "top" at $y = 1$. Note that the parabola $y = ax^2$, has curvature $2a$ at its vertex, so that when sweeped it generates a ridge and a corresponding A_3 curve (rim), Figure 12. By a modification, we can make this parabola bulge in the middle while keeping $z = \pm 1$ sections constant. $y = \left[a_1(1 - z^2) + a_2z^2\right] x^2$, so that at $z = 0$, the curvature of the cross section is $2a_1$, while at $z = \pm 1$ the curvature of the section is $2a_2$. Alternatively, one can close up the graph $y = a_1x^2$ with a "top" $y = a_2z^2$, as illustrated in Figure 12, middle row.

6) The $A_1^2A_3$-II Transition: This transition describes the interaction of a ridge curve endpoint A_1A_3 with a distinct central axis curve A_1^3. The ridge initially "hangs off" a "central" portion of some medial axis sheet, as generated by the A_1A_3-I example (the only way to generate a new ridge!). The latter sheet typically intersects two other sheets at an A_1^3 curve. Now, as the ridge is moved so that its corresponding endpoint A_1A_3 on the medial axis moves towards the latter A_1^3 axis, it is possible for the two to interact at some point. Since the end points of a rim are A_1A_3 points, we expect these to approach the A_1^3 curves transversally. At the point of collision the A_1A_3 contact sphere of the rim-end encounters the third boundary surface (*i.e.,* the third contact in the A_1^3 curve not represented by the A_1^2 sheet). Thus, it becomes an $A_1^2A_3$ contact point joining

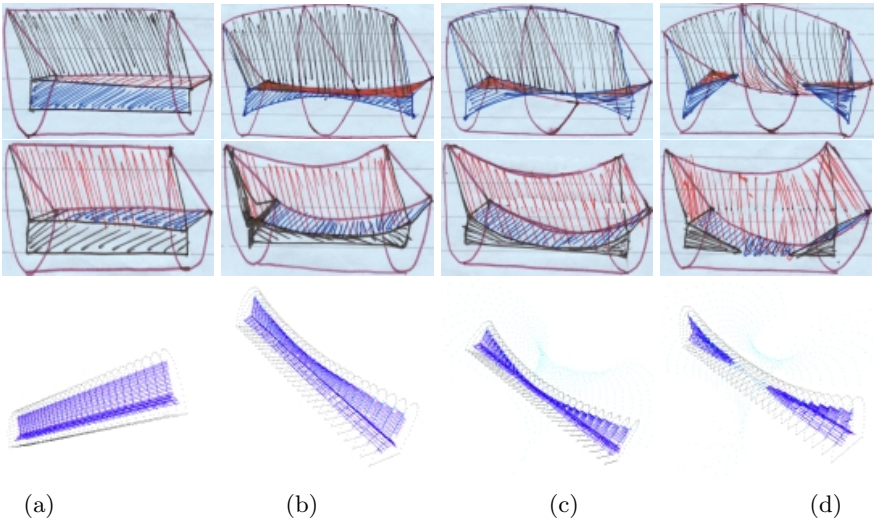

Fig. 12. (Top row) : The flattening of the central portion of this parabolic shape moves the ridge-related A_3 curve (rim) up towards the central axis A_1^3 curve until they collide at an A_1A_3-II transition. After this point the A_1^3 and A_3 curves both split into two pieces joined at two newly formed A_1A_3 points. Note that the medial axis between these points is a smooth A_1^2 sheet. (Middle Row): An alternate form. (Bottom Row) : The simulation of the medial axis evolution showing the Perestroika at an A_1A_3-II point.(Simulations from [12]).

the A_3 and A_1^3 curves corresponding to the ridge and its base, respectively, with the two A_1^3 half portion of the original A_1^3 curves. After this point, as the ridge is pushed further along, the A_3 contact of the ridge pairs off with the newly acquired A_1 contact and form an A_1A_3. The $A_1^2A_3$ contact becomes tangent at the original three points and the sides of the ridge for an A_1^4 contact. Four A_1^3 curves come together at this point, Figure 13.

A shape which gives rise to this transition can be constructed as follows: consider the shape used in Figure 8, generated by Equation 2, or the parabolic "gutter" in Figure 12. Create a bump using the A_1A_3-I transition by adding a Gaussian, Equation 1, in the central portion of the shape. We give this bump a random orientation θ,

$$y(x,z) = Ae^{\frac{-(x\cos(\theta)+z\sin(\theta))^2}{2\sigma_1^2}} e^{\frac{-(-x\sin(\theta)+z\cos(\theta))^2}{2\sigma_2^2}}. \quad (3)$$

The bump can then be placed on the surface and positioned roughly on the central portion, Figure 13, and then moved until its base on the medial axis (the A_1^3 curve generated by the bump) collides with the A_1^3 curve of the main shape, Figure 13(b). Thereafter, the base is split into two segments one on each of the corresponding sheets of the A_1^3 curve. The simulation using a parabolic gutter is shown in Figure 14.

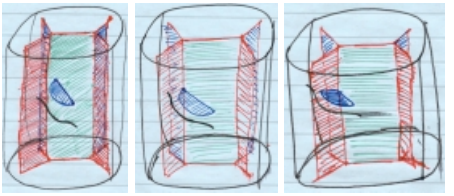

Fig. 13. The $A_1^2A_3$-I transition. A "bump" (blue) is placed so that it modifies the central sheet of the medial axis (green). As the bump is moved left towards the A_1^3 curve on the left side of the object, the A_1A_3 point of the bump eventually hits the A_1^3 axis creating an $A_1^2A_3$ transition. Beyond this point the "base" of the bump is on two distinct sheets.

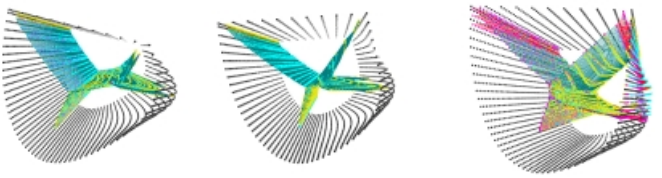

Fig. 14. Example of Perestroika with an $A_1^2A_3$-I point.(Simulations from [12]).

7) The $A_1^2A_3$-II Transition : This transition describes the process of creating a ridge whose base is on an A_1^3 medial axis curve itself, as opposed to the central portion of an A_1^2 sheet, *i.e.,* in creating the ridge in the A_1A_3 transition, the A_1A_3 medial point arises not on an A_1^2 sheet but on the A_1^3 curve.

This transition is related to the previous $A_1^2A_3$-I transition, but instead of using an A_1A_3 transition to generate a ridge positioned on a medial sheet and then moved to collide with the A_1^3 axis, it is generated and then moved right on the A_1^3 axis. A shape deformation corresponding to this transition then applies an A_1A_3 transition of the form of Equation 3 but positioned on one of the true constant curves of the A_1^3 medial curve on the surface, with the amplitude increasing. Initially when A is small, the effect is to perturb the A_1^3 axis slightly. But with increasing A the transition is reached, and finally the ridge becomes apparant as the rightmost figures in Figures 13 and 14.

Acknowledgments. We gratefully acknowledge the support of NSF grants BCS-9980091 and ECS-0070887. We also appreciate the assistance of Mireille Boutin, Frederic Leymarie and Raghavan Dhandapani in creating some example cases and in the preparation of this document.

References

1. I. A. Bogaevski. Singularities of viscosity solutions of Hamilton-Jacobi equations. 2001.

2. I. A. Bogavski. Metamorphoses of singularities of minimum functions and bifurcations of shock waves of the Burgers Eq. with vanishing viscosity. *Math. J.*, 1(4):807–823, 1990.
3. J. Bruce and P. Giblin. *Curves and Singularities*. Cambridge University Press, 1984.
4. J. Bruce, P. Giblin, and C. Gibson. Symmetry sets. *Proceedings of the Royal Society of Edinburgh*, 101A:163–186, 1985.
5. P. J. Giblin and B. B. Kimia. On the local form of symmetry sets, and medial axes, and shocks in 3D. Technical Report LEMS-171, LEMS, Brown University, May 1998.
6. P. J. Giblin and B. B. Kimia. On the local form and transitions of symmetry sets, and medial axes, and shocks in 2D. In *ICCV* , pages 385–391, KerKyra, Greece, Sept. 1999.
7. P. J. Giblin and B. B. Kimia. On the local form of symmetry sets, and medial axes, and shocks in 3D. In *Proceedings of CVPR*, pages 566–573, Hilton Head Island, South Carolina, USA, June 13-15 2000. IEEE Computer Society Press.
8. P. J. Giblin and B. B. Kimia. On the local form and transitions of symmetry sets, medial axes, and shocks. *IJCV*, Submitted, March, 2001.
9. P. L. Halliman, G. G. Gordon, A. L. Yuille, P. Giblin, and D. Mumford. *Two- and Three-Dimensional Patterns of the Face*. A. K. Peters, 1999.
10. M. S. Johannes, T. B. Sebastian, H. Tek, and B. B. Kimia. Perceptual organization as object recognition divided by two. In *Workshop on POCV*, pages 41–46, 2001.
11. L. Lam, S.-W. Lee, and C. Y. Suen. Thinning methodologies-a comprehensive survey. *IEEE Trans. on PAMI*, 14(9):869–885, September 1992.
12. F. F. Leymarie. *3D Shape Representation via Shock Flows*. PhD thesis, Brown University, 2002.
13. R. L. Ogniewicz and O. Kubler. Hierarchic voronoi skeletons. *Pattern Recognition*, 28(3):343–359, 1995.
14. T. B. Sebastian, P. N. Klein, and B. B. Kimia. Recognition of shapes by editing shock graphs. In *Proceedings of the Eighth International Conference on Computer Vision*, pages 755–762, Vancouver, Canada, July 9-12 2001. IEEE Computer Society Press.
15. D. Shaked and A. M. Bruckstein. Pruning medial axes. *Computer Vision and Image Understanding*, 69:156–169, 1998. 2.
16. S. Tari and J. Shah. Extraction of shape skeletons from grayscale images. *Computer Vision Image Understanding*, 66(2):133–146, 1997.
17. H. Tek and B. B. Kimia. Boundary smoothing via symmetry transforms. *Journal of Mathematical Imaging and Vision*, 14(3):211–223, May 2001.